Matériaux & Techniques **114**, 308 (2026)

https://doi.org/10.1051/mattech/2026017

Matériaux & Techniques

Special Issue on 'Opportunities and Challenges of Hydrogen Use for Steelmaking Decarbonization', edited by Ismael Matino, Valentina Colla and Akhilesh Swarnakar

Available online at: www.mattech-journal.org

ORIGINAL ARTICLE

OPEN ACCESS

Effect of Hydrogen as fuel for continuous annealing of AISI 316L stainless steel—annealing and pickling tests

Eugenia Sainsus, Lorenza Catini, Niccolò Massarelli, and Baldo Gurreri

RINA Consulting – Centro Sviluppo Materiali S.p.A., Roma 00128, Italy

Received: 23 December 2025 / Accepted: 30 March 2026

Abstract. This work explores the replacement of natural gas with hydrogen as the combustion fuel in free-flame continuous heat treatment furnaces for stainless steel strip, focusing on its influence on oxide scale formation and removal in AISI 316L steel. The higher water vapor content of hydrogen combustion atmospheres may alter the oxide scale's composition, thickness, and adherence, potentially affecting downstream descaling and pickling processes. To assess these effects, both cold- and hot-rolled AISI 316L samples were annealed and oxidized in 100% CH_4 and 100% H_2 combustion atmospheres under three different thermal cycles. The resulting oxide layers were analyzed through SEM, EDX, and GDOES to determine their morphology and chemical composition, followed by comparative evaluation of the descaling behavior and minimum pickling times.

Results indicate that annealing in both methane and hydrogen fumes modifies the scale of hot-rolled materials, leading to oxidation and spallation. Hydrogen fumes promote spallation, primarily forming Fe_3O_4 and Fe_2O_3 powder, while chromium depletion remains unaffected by the atmosphere. For hot rolled material, annealing in hydrogen fumes tends to reduce or leave the pickling time unchanged and to increase the shot blasting weight loss compared to natural gas.

In cold-rolled 316L, oxide thickness increases with temperature and is constantly greater in hydrogen fumes due to water vapor-induced chromium evaporation. Iron oxide clusters observed at high temperatures suggest the beginning of breakaway oxidation, though not fully developed under the tested conditions. Annealing in hydrogen fumes similarly reduces or does not influence the pickling time and does not affect overall weight losses. These findings support the potential of hydrogen as a sustainable fuel alternative without detrimental effects on surface quality or processing efficiency.

Keywords: annealing / pickling / scale / oxidation / stainless steel / hydrogen

1 Introduction

Stainless steels (SS) are alloys consisting mainly of iron and chromium at a concentration higher than 10.5%, which gives the material its chemical resistance thanks to the formation of the well-known protective Cr_2O_3 passivation layer [1,2]. Nickel, which is added to stabilize the austenitic phase at room temperature, is also one of the main alloying elements [3]. During 2024, a total of 62,620 kt of stainless steel was produced worldwide [4], out of which 27,000 t were coils of austenitic stainless steel.

Coils of stainless steel require annealing, both in the hot-rolled (HR) and cold-rolled (CR) states, to acquire the desired mechanical and chemical properties and the desired surface appearance. The most common way of heating the strip to obtain the desired thermal treatment is through continuous annealing furnaces powered by free flame burners [5] in which natural gas (NG), which is essentially methane, is used as fuel. Excess air is usually employed as the comburent according to the reaction:

$$CH_4 + \lambda(2O_2 + 7.52N_2) \rightarrow CO_2 + 2H_2O + 7.52\lambda N_2 + 2(\lambda - 1)O_2.$$

Due to the oxidizing nature of combustion fumes, and due to the presence of a preexisting oxide scale for HR coils, pickling is also usually requested after annealing.

Annealing is the main source of Scope 1 GHG (greenhouse gas) emissions in the cold rolling area, leading to emissions of up to 132 kg of CO_2 equivalent per ton of finished cold-rolled steel; therefore, the substitution of NG with H_2 as fuel could be a suitable way of reducing the carbon footprint of stainless steel production with minimal modification to treatment line furnaces.

However, while the combustion of NG yields an atmosphere containing a maximum water content of 19 mol%,

* e-mail: niccolo.massarelli@rina.org

Table 1. AISI 316L stainless steel chemical composition (wt%).

Steel grade	C	Cr	Ni	Mo	Si	Mn	Cu
AISI 316L	0.03	16.7	10.3	2.1	0.34	1.3	0.4

the combustion of H_2 leads to a maximum water content of 34mol%, and since H_2O is known to have oxidizing effects on metals and alloys, a substantial impact on surface oxidation cannot be ruled out [6].

Some scientific literature is available on annealing in methane fumes. In [7], the authors performed annealing tests at various treatment times for cold-rolled samples, finding that some chromium evaporation occurs during annealing, but a top layer of manganese chromite forms after some time, blocking Cr(VI) evaporation. The authors also observe boron enrichment at the scale-metal interface. The study in [8] confirms that most austenitic stainless steels (AISI 304 and 316L) are unable to form a layer of Cr_2O_3, which could protect from high-temperature oxidation (in accordance with Wagner's [9] theory). The conclusions obtained by [10] for cold-rolled 304 stainless steel are that increasing annealing temperature makes descaling easier and that O_2 up to 2% vol. in the atmosphere has the effect of reducing oxidation. For hot-rolled products, the authors conclude that annealing has practically no effect on scale characteristics.

An interesting part of the scientific literature deals with chromium(VI) vaporization in water-rich atmospheres. The main conclusions reached in [11] are that at low water percentages CrO_3 evaporation occurs, while at higher water partial pressures $CrO_2(OH)_2$ is the main evaporating species. The authors of [12] observe that, while in dry O_2 the ferritic SS studied is able to form a protective layer of Cr_2O_3, when water is added, the evaporation of chromic acid makes the atmosphere more corrosive, leading to breakaway oxidation. In [13], a mechanism involving $CrO_2(OH)_2$ evaporation, which leads to the formation of iron oxide nodules during oxidation in humid air, was proposed.

Recent developments in the field of H_2-fueled annealing of stainless steel focus on oxi-combustion of hydrogen, leading to annealing atmospheres containing 95% H_2O. The study of Airaksinen et al. [14], focused on annealing of cold-rolled 441 and 304, pointed to a higher oxidizing power of the H_2 oxy-combustion atmosphere compared to the CH_4 oxy-combustion atmosphere. An earlier onset of breakaway oxidation and the formation of Fe-rich oxide nodules were also observed when switching to H_2. No published literature is yet available concerning the picklability of 316L stainless steel after annealing in H_2 fumes. In [15], although part of the tests was carried out at treatment times longer than the typical annealing time, the conclusion was that 316L always shows signs of breakaway oxidation when annealing in humid air.

For what concerns the role of Mo during oxidation of cold-rolled 316L, a study [16] proposes that Mo, while being significantly less noble than Ni [17,18] enriches at the scale-metal interface and plays a protective role hindering iron diffusion outwards and improving scale adherence.

The purpose of this work is to assess whether the substitution of NG in favor of H_2 could influence annealing, pickling, and the final properties of the steel through a different surface oxidation occurring during continuous annealing. To assess this possibility, annealing followed by descaling and pickling was simulated on a laboratory scale for both NG-fueled and H_2-fueled processes.

2 Material and methods

2.1 Material selection and characterization

This work focuses on austenitic stainless steel of AISI 316L grade, whose samples were supplied by Marcegaglia Gazoldo Inox in both hot-rolled and cold-rolled finishing. The chemical composition of the AISI 316L steel grade is presented in Table 1, meeting the specifications for this grade with a chromium content of 16.7 wt% and a nickel content of 10.3 wt%, which, together with a high Mo content, are characteristic of this austenitic stainless-steel grade.

The hot-rolled samples were supplied with a thickness of 3.0 mm, while the cold-rolled samples had a thickness of 1.50 mm. These thicknesses were selected to represent typical industrial flat products subjected to continuous annealing processes.

Firstly, the HR material has been characterized in an "as received" state using scanning electron microscope (SEM) and energy dispersive X-ray spectroscopy (EDX) techniques (Figs. 1 and 2, respectively). The surface appeared oxidized and with a compact scale adherent to the base alloy with an average scale of 10 μm. The EDX analysis shows a scale rich in chromium oxide at the scale-metal interface and iron-rich scale on the outer layers.

2.2 Sample preparation

All samples were cut from the supplied sheets into rectangular specimens measuring 40 × 80 mm, with the longer side aligned parallel to the rolling direction to keep consistent direction during subsequent testing. This geometry was standardized to facilitate loading into the horizontal tubular furnace (see Fig. 3) and to enable reproducible thermal cycling conditions throughout the experimental campaign.

Prior to thermal treatment, all cold-rolled samples underwent a degreasing treatment to remove residual rolling oils and other manufacturing residues that might otherwise interfere with oxide layer formation.

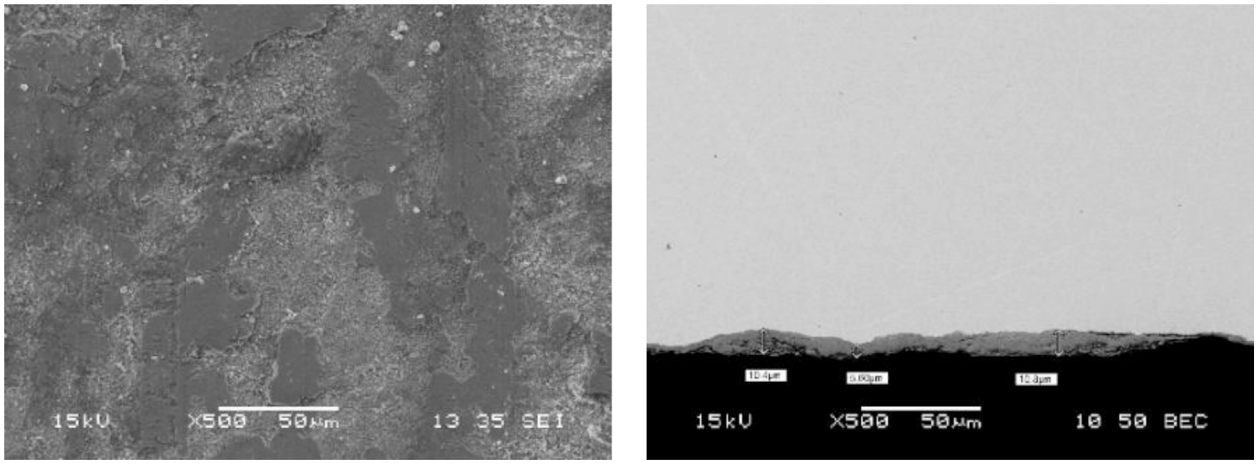

Fig. 1. Characterization of the hot-rolled 316L "as received". (a) SEM surface analysis. (b) SEM section analysis.

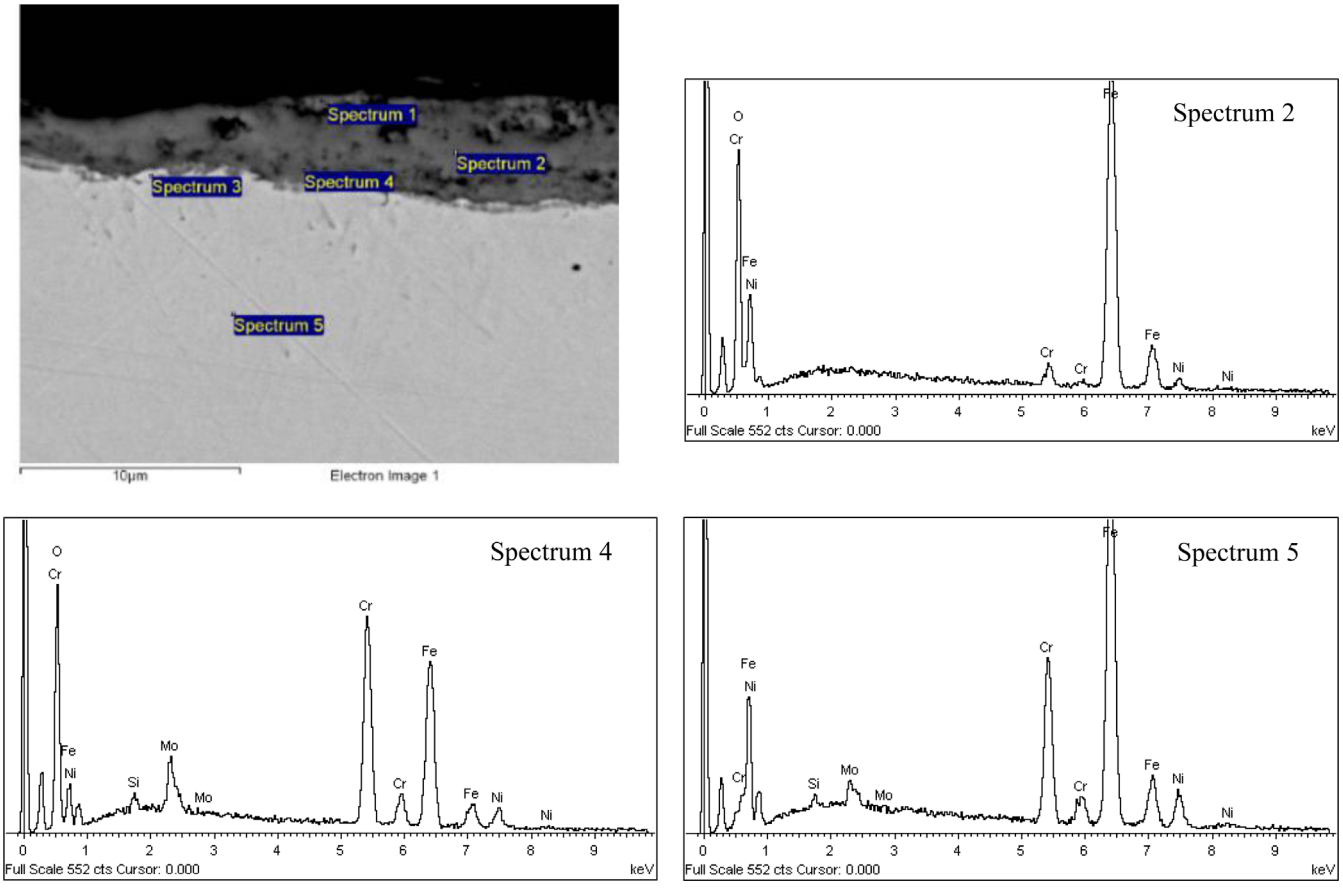

Fig. 2. EDX section analysis of the hot-rolled 316L "as received".

2.3 Annealing equipment and thermal cycling

All annealing experiments were conducted in a horizontal tubular furnace whose schematic representation is reported in Figure 3 and is equipped with two independently controlled heating zones. The furnace design allows for samples to be inserted on a dedicated sample holder, which can be precisely positioned within the high-temperature zone via a rail-guided mechanical system. This configuration enables rapid insertion and extraction of samples and facilitates controlled cooling following thermal treatment.

2.4 Thermal cycles and annealing conditions

Two distinct annealing atmosphere compositions were investigated, each representing a different combustion environment relevant to industrial heat treatment applications. The first atmosphere consisted of artificial fumes that simulated natural gas (which was assumed to be pure methane) combustion fumes obtained with an excess air of 18% (air–fuel ratio of 1.18), while the second consisted of hydrogen combustion products with the same air–fuel ratio of 1.18. The resulting annealing atmosphere compositions are summarized in Table 2.

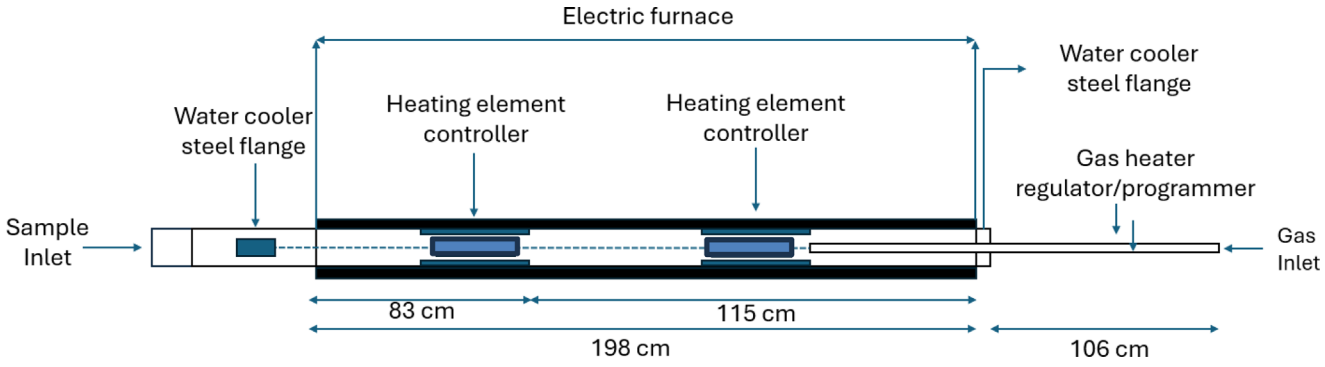

Fig. 3. Two-zone horizontal tubular furnace.

Table 2. Composition of the annealing atmosphere which simulate the combustion of methane and hydrogen.

Component	Methane combustion	Hydrogen combustion
O_2 [mol%]	2	2
CO_2 [mol%]	9	0
H_2O [mol%]	18	32
N_2 [mol%]	71	66

The hydrogen combustion atmosphere is characterized by significantly elevated water vapor content (32 mol%) compared with methane combustion (18 mol%), while the CO_2 is missing.

For AISI 316L, three distinct thermal cycles were applied to both hot-rolled and cold-rolled samples. These cycles were designed to simulate three operational scenarios encountered in industrial continuous annealing lines:

- A cycle at the standard operating practice (SOP) temperature, representing normal production conditions for this steel grade.
- A cycle above the SOP temperature, representing over-annealing conditions at which excessive thermal treatment may occur.
- A cycle below the SOP temperature, representing under-annealing conditions at which incomplete thermal treatment may occur.

The thermal cycles carried out for hot-rolled and cold-rolled materials are represented in Figures 4 and 5, respectively

Following thermal treatment, each annealed sample was analyzed using SEM and EDX to characterize the surface morphology and cross-sectional structure of the oxide scale formed during annealing and to determine the elemental composition of oxide phases formed during the annealing process.

To investigate the chromium depletion phenomenon in HR and CR 316L stainless steel, the EDX mapping and GDOES analysis were performed.

2.5 Pickling test

The annealing was followed by scale removal processes, simulated according to the industrial procedure [19]. The hot-rolled materials were subjected to shot blasting followed by chemical descaling and pickling, while the cold-rolled materials were descaled with an electrolytic process followed by chemical pickling.

The hot-rolled materials were first subjected to shot blasting using a laboratory-scale shot blasting machine. The process employed S110 spherical grit, compliant with SAE J444:1984, with a hardness of 40–50 HRC and a shot velocity of 70 m/s.

The optimal duration was determined through preliminary calibration, in which samples were treated at fixed 30-second intervals to monitor weight loss and identify the point at which the time-weight loss increment became negligible, as shown in Figure 6. The calibration was performed on material annealed in methane combustion fumes at SOP temperature. The resulting duration of 60 seconds was then applied to all samples annealed in both CH_4 and H_2 atmospheres, enabling a direct comparison of the data resulting from pickling.

Shot blasting of the hot-rolled samples was followed by a chemical descaling stage using sulfuric acid and, subsequently, by a final pickling step with a mixed acid solution containing hydrofluoric acid (HF) and sulfuric acid (H_2SO_4). Detailed parameters are provided in Table 3.

The pickling of cold-rolled materials was carried out through a multi-stage process. Initially, the oxide layer was conditioned by electrolytic pickling in a sulfuric acid solution under direct current, simulating the industrial conditions in which the strip is alternatively polarized in the anodic and cathodic states. Following this, chemical pickling was performed using a mixed acid solution composed of hydrofluoric acid and sulfuric acid. Detailed process parameters are provided in Table 4.

For both the hot- and cold-rolled samples, the minimum pickling time was determined through a visual assessment protocol consisting of the following steps: an initial pickling test was conducted using a starting time (corresponding to the industrial pickling time). The effectiveness of pickling was evaluated visually, and the duration was adjusted, either increased or decreased, based on the observed results. The samples were considered successfully pickled once there were no visible traces of residual oxides and the surface quality was comparable to the one obtained industrially. In any case the ratio between the residence time in Tank 1 and Tank 2 was kept constant to simulate the residence time of an industrial pickling

Combustion atmosphere	T [°C]	$t_{soaking}$ [s]	t_{TOT} [s]
CH_4	1150 (SOP)	21	90
	1080	-	110
	1190	42	133
H_2	1150 (SOP)	21	92
	1080	-	112
	1190	21	135

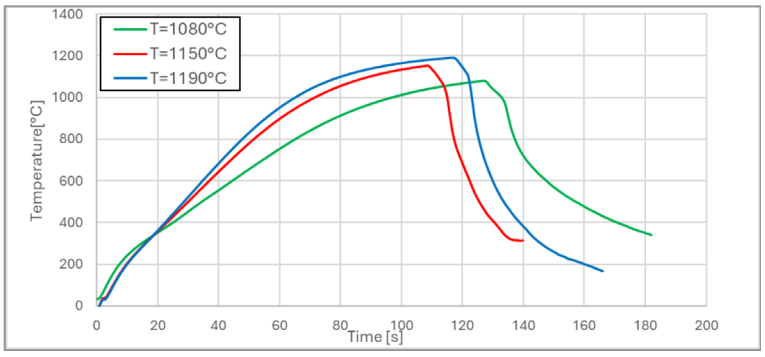

Fig. 4. Annealing thermal cycles to be applied to hot-rolled 316L stainless steel samples.

Combustion atmosphere	T [°C]	$t_{soaking}$ [s]	t_{TOT} [s]
CH_4	1140 (SOP)	24	94
	1180	48	104
	1080	-	90
H_2	1140 (SOP)	24	95
	1180	48	103
	1080	-	93

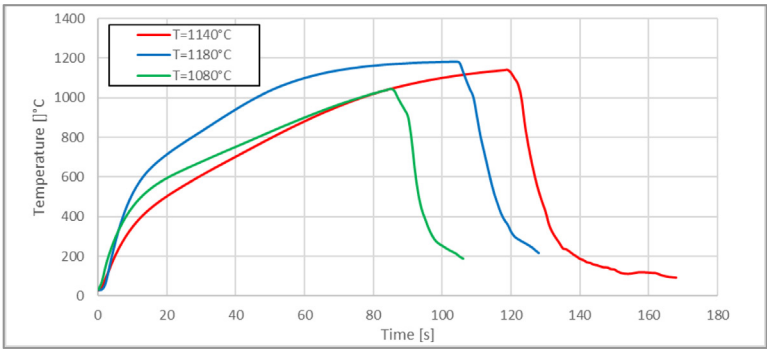

Fig. 5. Annealing thermal cycles to be applied to cold-rolled 316L stainless steel samples.

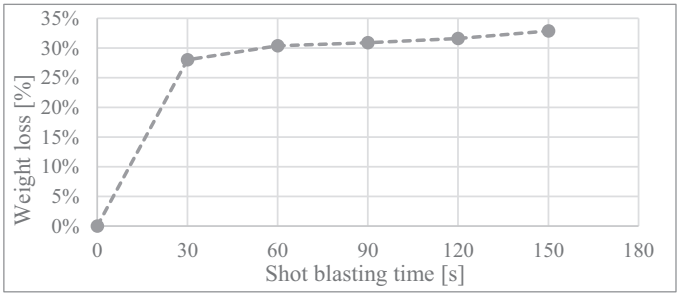

Fig. 6. Weight loss (%) as a function of shot blasting time(s) for hot-rolled 316L steel grade annealed in methane combustion fumes.

section. The final minimum effective pickling time was confirmed through two repeated tests to validate the outcome.

Pickling time was also validated by SEM observation of the sample surfaces, allowing also to evaluate possible differences in surface morphology of the pickled samples.

3 Results

3.1 Annealing scale characterization

Tables 5 and 6 present the findings from the SEM analysis on both HR and CR samples. Analyses were performed on the cross-sections of HR samples after exposure to each thermal cycle and on the surface of the CR due to the thin nature of the oxides.

Table 3. Pickling bath composition for hot-rolled finishing of 316L steel grade.

Pickling tank	Components	Concentration [g/L]	T [°C]
Tank 1	H_2SO_4	200	90
Tank 2	Fe^{3+}	40	60
	HF	35	
	Fe^{2+}	25	
	H_2SO_4	120	

For hot-rolled 316L annealed in CH_4 fumes, the oxide scale thickness ranges from about 9 to 13 µm depending on temperature and is generally thicker and less adherent than

Table 4. Pickling bath composition for cold rolled finishing of 316L steel grade.

Pickling tank	Components	Concentration [g/L]	Current density [A/dm^2]	T [°C]
Tank 1	H_2SO_4	100	8	50
	Fe^{2+}	15		
Tank 2	Fe^{3+}	40	–	30
	HF	35		
	Fe^{2+}	25		
	H_2SO_4	120		

Table 5. SEM analysis on the cross-section of AISI 316L HR annealed in methane and hydrogen combustion fumes.

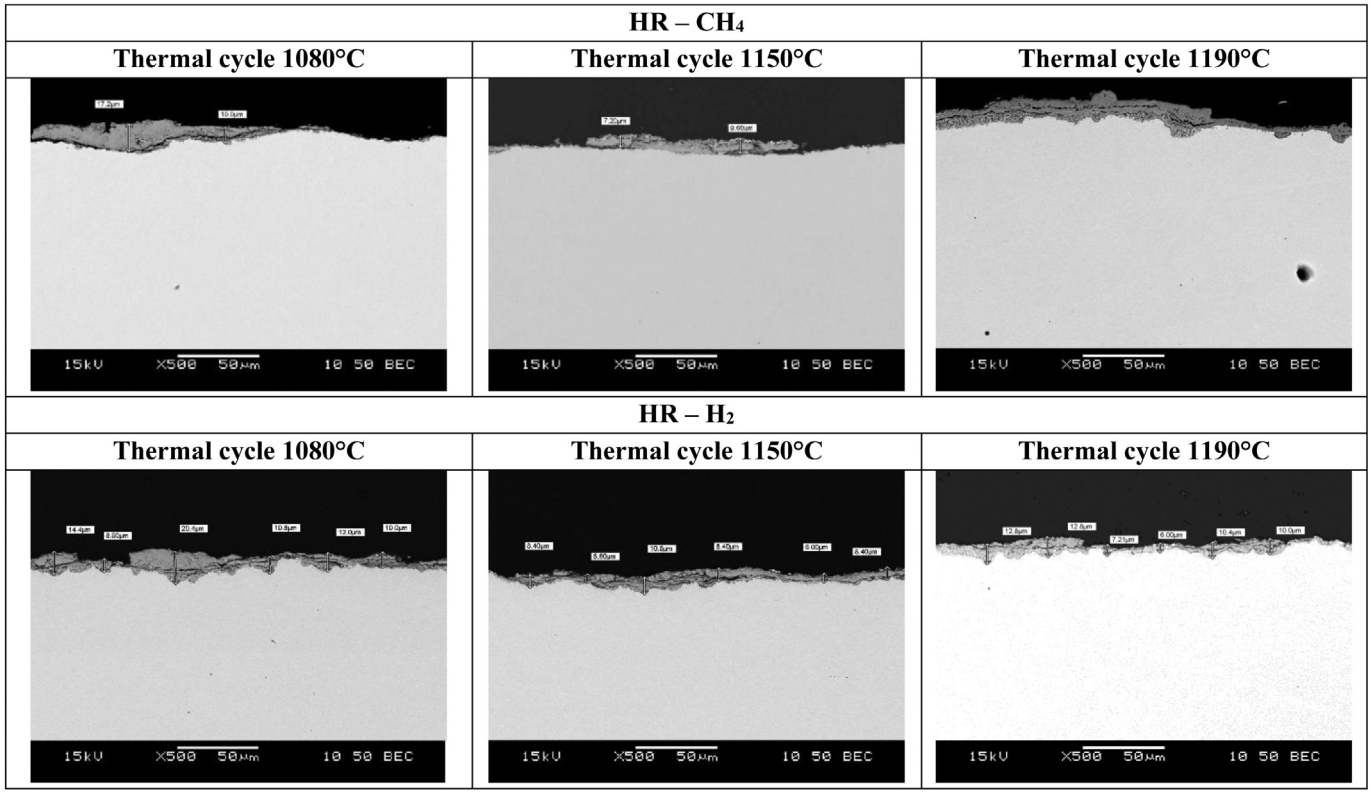

on as-received material. The scale is porous and, where locally detached, reveals a chromium-rich underlying layer. Cross-sectional observations indicate an inner chromium-rich oxide at the scale–metal interface, gradually transitioning to an iron-rich outer region, consistent with the alloy composition. At the highest temperature, chromium-rich oxides penetrate a few micrometers into the substrate as heterogeneous Fe–Cr oxide regions within the metallic matrix. Internal oxidation, in the form of oxide globules and channels, is present at all temperatures. Nickel-rich inclusions are detected at the interface and within the scale.

For hot-rolled 316L annealed in hydrogen fumes, the scale thickness depends on temperature and is between 8 and 13 µm. The scale is generally adherent, although significant detachment during annealing affects the reliability of thickness measurements. In fact, massive-scale detachment in the form of powder was observed during cooling. Through X-ray diffraction (XRD) analysis, the composition of this powder was found to be solely iron oxides (reported in Fig. 7). The interfacial oxide is enriched in chromium, manganese, and silicon, becoming more iron-rich toward the gas side. At higher temperatures, zones containing oxide globules dispersed in a nickel-rich matrix develop near the interface. Internal oxidation is again observed.

In cold-rolled 316L, both CH_4 and H_2 fume annealing lead to very thin but largely continuous scales that preserve the grain boundary "memory" of the substrate. Grain boundaries are highlighted by chromium-enriched smudges, and at higher temperatures, scale detachment exposes metallic areas with reduced chromium content, indicating chromium depletion. When

Table 6. SEM analysis on the surface of AISI 316L CR annealed in methane and hydrogen combustion fumes.

CR – CH_4		
Thermal cycle 1080°C	**Thermal cycle 1140°C**	**Thermal cycle 1180°C**
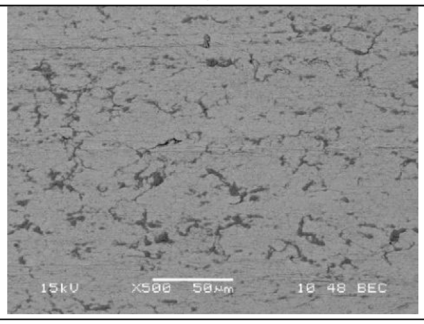	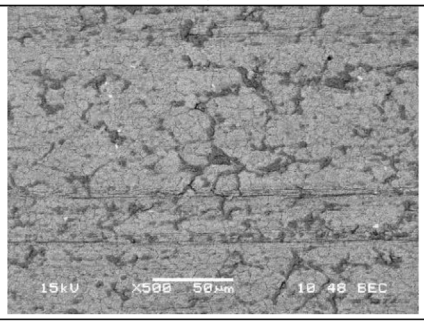	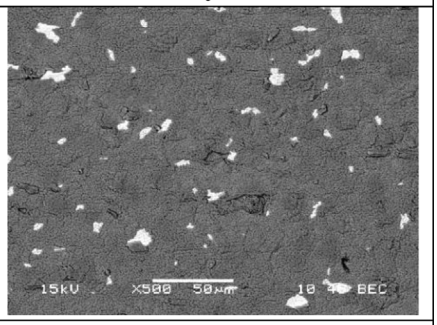
CR – H_2		
Thermal cycle 1080°C	**Thermal cycle 1140°C**	**Thermal cycle 1180°C**
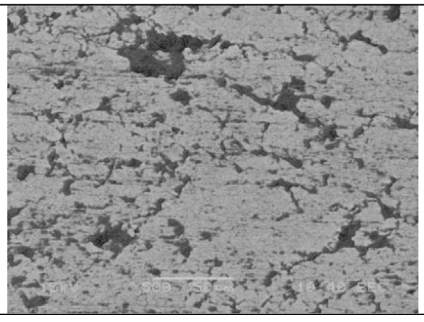	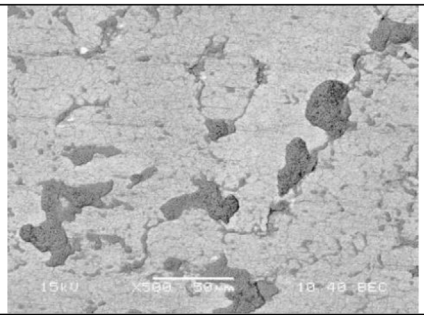	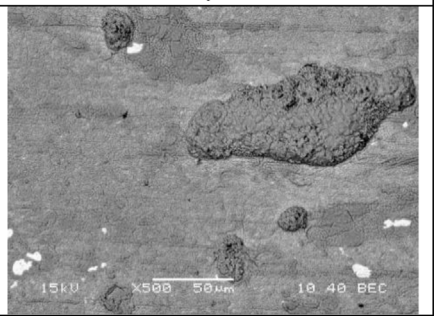

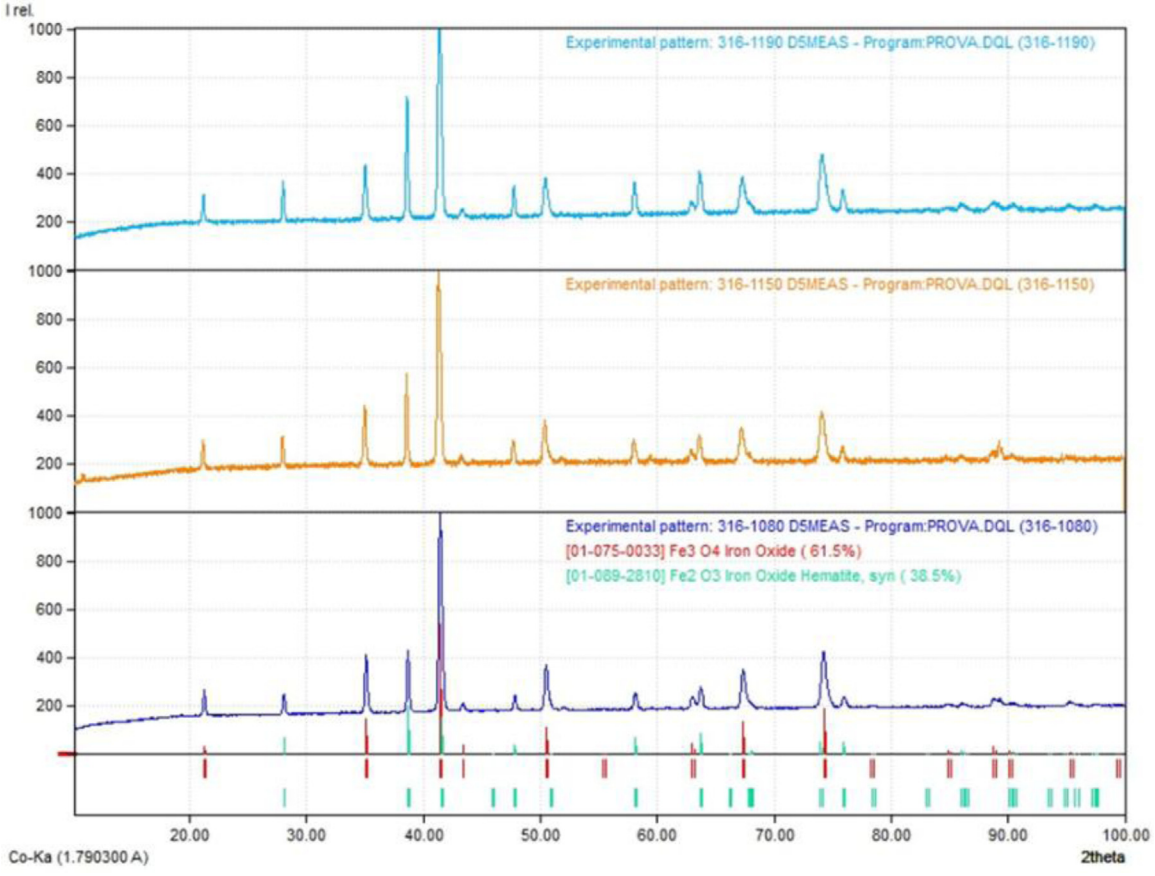

Fig. 7. XRD diffractogram of the oxide powder detached during H_2 fumes annealing.

Table 7. Analysis of chromium depletion in 316L stainless steel annealed at 1150°C in different annealing atmosphere.

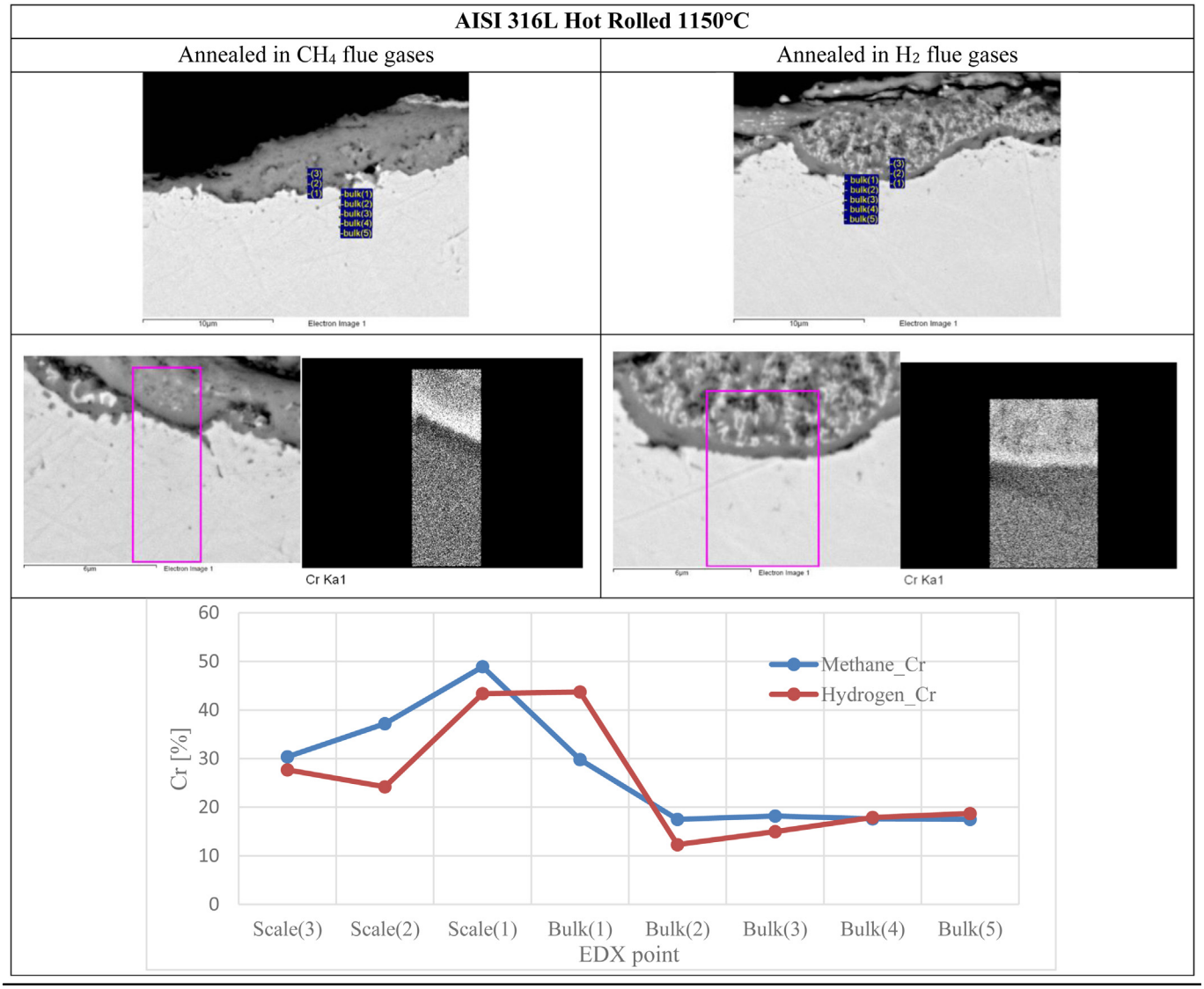

annealing in H_2 combustion fumes at intermediate and elevated treatment temperatures, iron oxide clusters appear on the surface, their dimension increasing with temperature.

Table 7 reports the results of the cross-section EDX and EDX mapping of the scale and bulk beneath the scale in order to identify element concentration distribution at the SOP condition for both annealing in methane and hydrogen fumes. The same analysis was also performed for the lowest and the highest treatment temperatures and is not reported for brevity.

From the EDX mapping and the EDX concentration profiles, a clear chromium-depleted layer was visible for all treatment conditions, reaching minimum Cr concentrations as low as 10% in some instances. No significant difference between the two annealing atmospheres was detected in terms of minimum chromium concentration or Cr-depleted layer thickness.

In the Figure 8, the results of quantitative Glow Discharge Optical Emission Spectroscopy (GDOES) analysis are reported for both methane and hydrogen fumes.

As the treatment temperature increases, the average scale thickness, which was determined by the minimum of Cr concentration, also increases-from approximately 0.7 microns at lower temperatures to about 1.7 µm at 1180°C. Additionally, a chromium depleted layer can be observed. For treatments in hydrogen combustion fumes, the chromium concentration of the Cr-depleted layer is always lower than that achieved during methane annealing.

3.2 Pickling tests results

The results of pickling tests carried out on hot-rolled samples annealed in CH_4 or H_2 combustion atmospheres are summarized in Table 8 and Figure 9. The data include

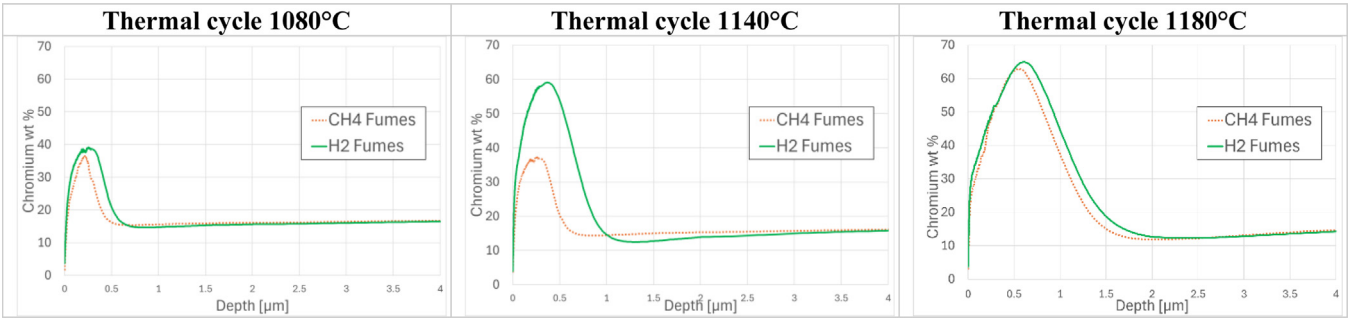

Fig. 8. Analysis of chromium depletion in 316L stainless steel annealed at 1080°C, 1150°C, and 1180°C.

Table 8. Average minimum pickling time and weight losses of hot-rolled samples annealed in CH_4 or H_2 combustion fumes at three different maximum temperatures.

Atmosphere	Maximum temperature [°C]	Minimum pickling time [s]	Shot blasting weight loss [g/m^2]	Pickling weight loss [g/m^2]	Total weight loss (shot blasting + pickling) [g/m^2]
CH_4 fumes	1080	90	22	62	84
	1150	90	30	51	80
	1190	135	31	89	120
H_2 fumes	1080	60	82	45	127
	1150	90	43	63	106
	1190	90	32	74	106

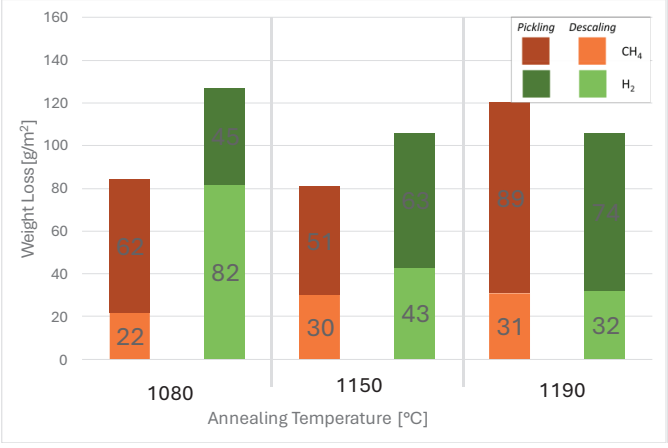

Fig. 9. Average weight losses of hot-rolled 316L samples annealed in CH_4 or H_2 combustion fumes at three different maximum temperatures.

the minimum pickling time and the corresponding average weight loss, expressed in g/m^2. To provide a comprehensive assessment of scale removal efficiency, the contributions from both shot blasting and pickling are also reported.

For the CH_4 fumes atmosphere, the lowest total weight loss was observed in samples annealed at 1150°C, with similar values at 1080°C. For these samples, the minimum pickling time remained constant at 90 s. The highest total weight loss occurred at 1190°C, which also corresponds to the longest minimum pickling time of 135 s.

Regarding the H_2 fumes atmosphere, the total weight loss reached its maximum at 1080°C, mainly due to a greater contribution from shot blasting and corresponds to the shortest pickling time. The total weight loss decreased at 1150°C and remained constant at 1190°C, although with a different distribution between shot blasting and pickling, with a higher effect of pickling at the highest annealing temperature. The pickling time remained constant at 1150°C and 1190°C.

Surface characterization of the pickled samples was conducted using SEM at 100× magnification (Fig. 10), confirming complete removal of oxide scale for the samples annealed in CH_4 or H_2 combustion fumes. EDX analysis (Fig. 11) further validated the pickling effectiveness, with very low oxygen peaks indicating successful pickling.

The results of pickling tests carried out on cold-rolled samples annealed in CH_4 or H_2 combustion atmospheres are summarized in Table 9. The data include the minimum pickling time and the corresponding average weight loss, expressed in g/m^2.

For the CH_4 fumes atmosphere, the total weight loss increased from the lowest to the intermediate annealing temperature and then remained nearly constant between the intermediate and the highest temperatures. The pickling time reached its maximum of 168 s for samples treated at the intermediate temperature, while it had a minimum of 68 s at the highest temperature.

Concerning the H_2 fumes atmosphere, weight loss increased with annealing temperature. The pickling time reached its maximum value of 84 s at 1140°C, while at both lower and higher annealing temperatures it was 68 s.

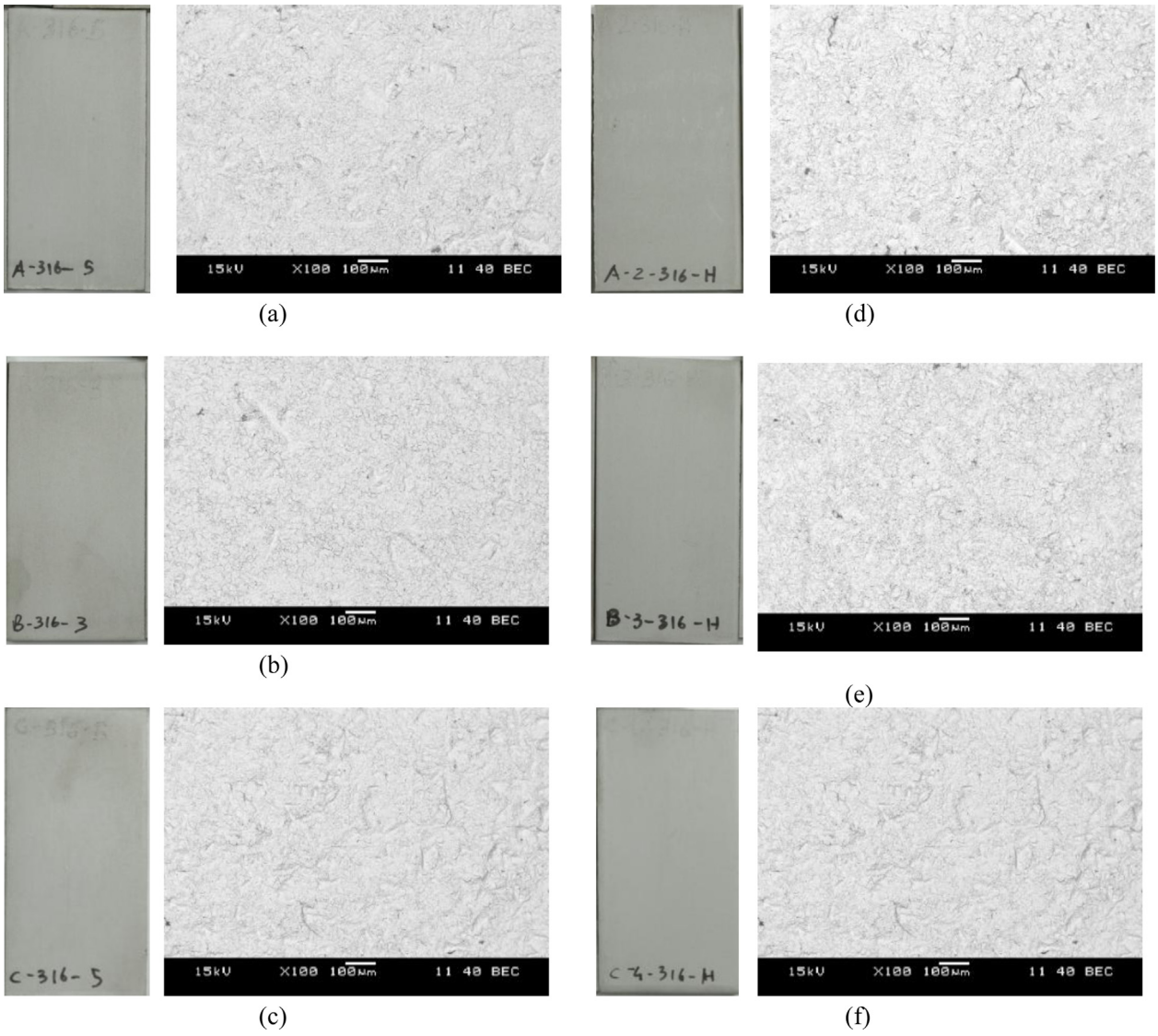

Fig. 10. Visual inspection and surface SEM analysis at 100× magnification after pickling treatment at minimum time of hot-rolled 316L samples annealed in atmosphere of CH_4 combustion fumes at maximum temperature of (a) 1080°C, (b) 1150°C, and (c) 1190°C and in atmosphere of H_2 combustion fumes at maximum temperature of (d) 1080°C, (e) 1150°C, and (f) 1190°C.

Figure 12 shows the samples treated at the minimum pickling time in CH_4 or H_2 combustion fumes atmosphere, appearing in both cases free of any macroscopically detectable residual oxide scale. For the samples annealed in CH_4, SEM analysis at 100× magnification reveals a modest presence of residual oxide scale on all three samples. Despite this, the scale was not detectable through standard visual inspection, which is the industrial practice, and the samples can therefore be considered effectively pickled. EDX analysis carried out on these samples (Fig. 13) indicates that the residual scale was primarily composed of oxides rich in Si and Mn that usually are more difficult to remove [19].

Regarding the samples annealed in H_2, SEM analysis at 100× magnification reveals the presence of residual oxide scale on the samples annealed at the maximum temperature of 1140°C. The EDX analysis reported in Figure 13 shows that the residual scale was mainly composed of oxides rich in Si and Mn that usually are more difficult to remove [19].

Further SEM analysis at 1500× magnification (Fig. 14) highlights signs of over-pickling within the steel matrix, suggesting that extending the pickling time could eliminate the remaining oxide scale but would likely compromise the luster of the substrate. In contrast, the sample annealed at

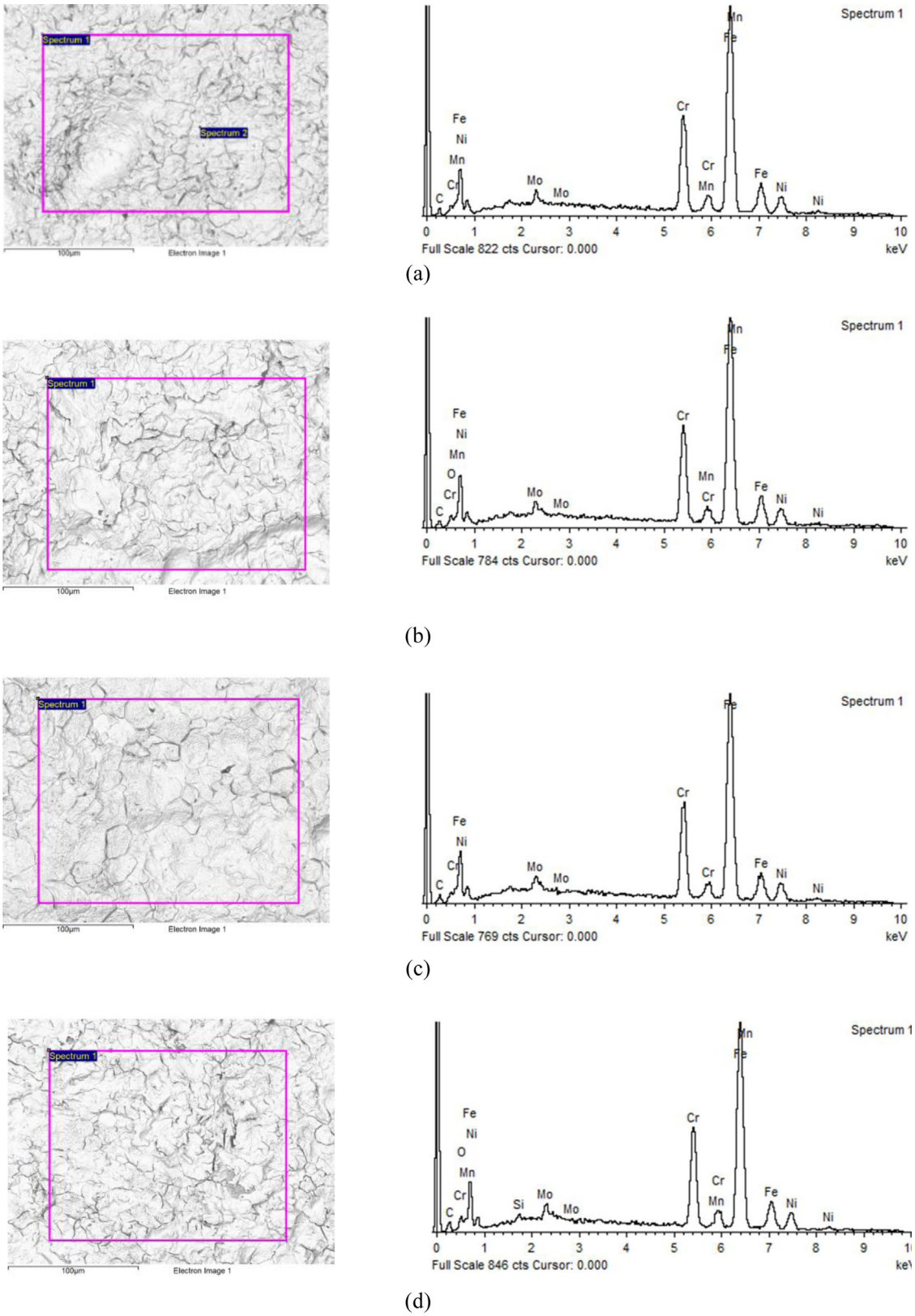

Fig. 11. EDX analysis after pickling treatment at minimum time of hot-rolled 316L samples annealed in atmosphere of CH_4 combustion fumes at maximum temperature of (a) 1080°C, (b) 1150°C, and (c) 1190°C and in atmosphere of H_2 combustion fumes at maximum temperature of (d) 1080°C, (e) 1150°C, and (f) 1190°C.

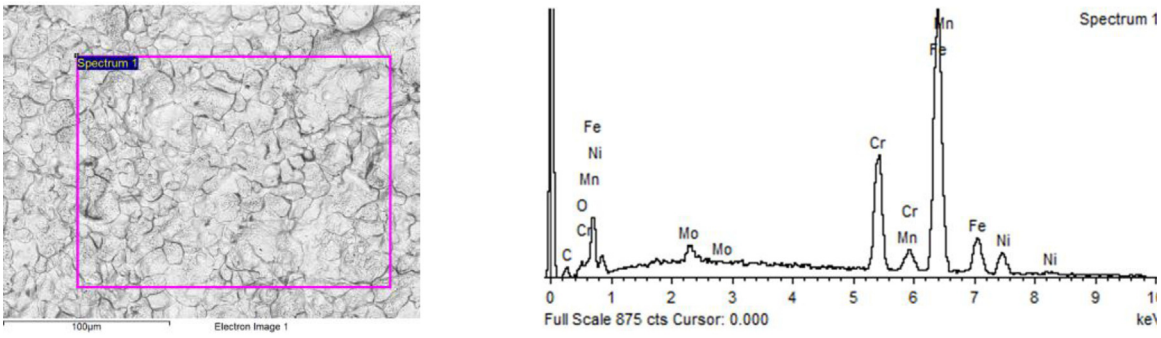

(e)

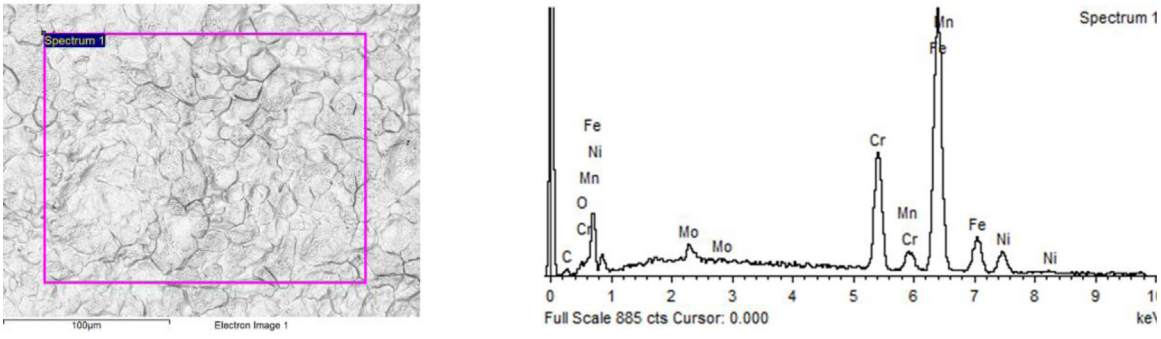

(f)

Fig. 11. (Continued)

Table 9. Average minimum pickling time and weight losses of cold-rolled samples annealed in both CH_4 and H_2 combustion fumes at different maximum temperatures.

Atmosphere	Maximum temperature [°C]	Minimum pickling time [s]	Pickling weight loss [g/m^2]
CH_4 fumes	1080	116	12
	1140	168	20
	1180	68	23
H_2 fumes	1080	68	12
	1140	84	20
	1180	68	28

1080°C exhibits only minor residual scale at 100× magnification, while the specimen treated at 1180°C appears free of residual scale.

4 Discussion

4.1 Hot-rolled samples

Both methane and hydrogen during annealing of HR 316L produce oxide scales of comparable thickness across the three thermal cycles. Scale thickness measurements reveal similar patterns in both environments: approximately 13 µm at lower temperatures and 9.4 µm (methane) and 8 µm (hydrogen) at the SOP temperature. At elevated temperatures, methane maintains 13 µm oxide thickness, while hydrogen reaches only 10 µm. This convergence at lower temperatures, followed by variance at higher temperatures, suggests that hydrogen fumes progressively favor the scale detachment.

Spallation phenomena were observed during the experimental campaign under both annealing in methane fumes and hydrogen combustion fumes. However, the phenomenon was significantly more pronounced during annealing in hydrogen combustion fumes. Scale spallation occurred during the cooling phase of the hot-rolled samples. An increment in oxide detachment at increasing temperatures was also observed. Analysis of the XRD diffraction patterns reveals that hematite (Fe_2O_3) and magnetite

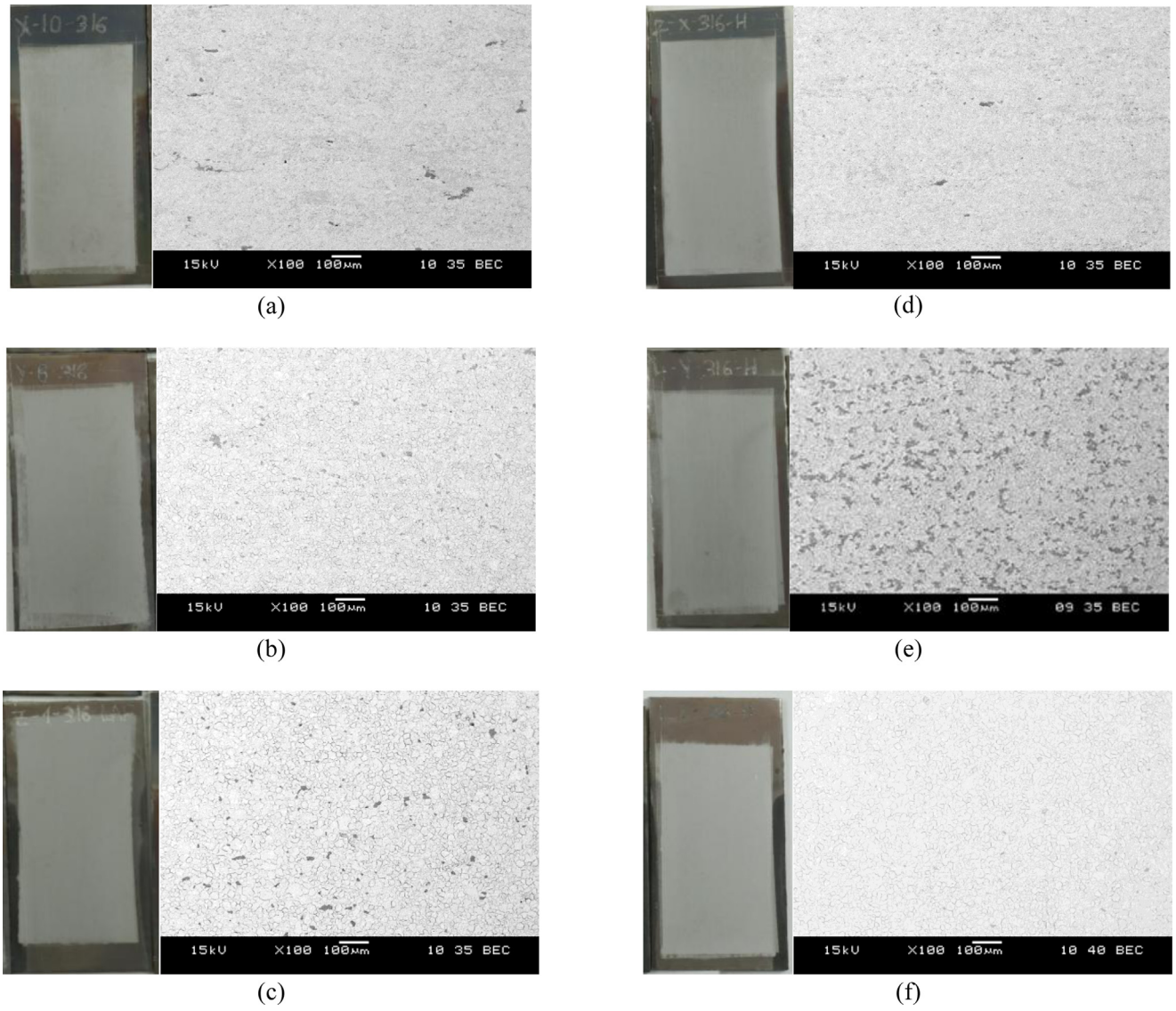

Fig. 12. Visual inspection and surface SEM analysis after pickling treatment at minimum time of cold-rolled 316L samples annealed in atmosphere of CH_4 combustion fumes at maximum temperature of (a) 1080°C, (b) 1140°C, and (c) 1180°C and in atmosphere of H_2 combustion fumes at maximum temperature of (d) 1080°C, (e) 1140°C, and (f) 1180°C.

(Fe_3O_4) are the only identified oxides, indicating the presence of only iron oxides in the collected powder samples. No chromium oxide phases were detected in any of the powder fractions. EDX identifies significant chromium presence within the scale, which remained attached to the samples. This difference between bulk-scale composition and powder composition indicates that chromium has likely vaporized as volatile species during the annealing process, leaving behind only iron oxides. Under oxidizing conditions, chromium volatilizes as $CrO_{3(g)}$, but the presence of water vapor substantially enhances this volatilization rate through hydroxide formation. The annealing conditions with elevated water vapor content promote the formation of volatile chromium oxy-hydroxide species, primarily $CrO_2(OH)_2$ [20]. This selective vaporization results in a chromium-depleted outer scale region dominated by iron oxides. The inner portion of the scale remains chromium-rich as can be noted in the EDX mapping. The experimental observations also reveal that chromium depletion in 316L stainless steel during annealing is influenced by temperature and less by annealing composition.

The use of hydrogen as a combustion fuel reduces the minimum pickling time at both the lower and higher maximum annealing temperatures. At the intermediate temperature, corresponding to typical industrial conditions, no significant difference was observed between the two atmospheres. At the lower and intermediate maximum temperatures, samples annealed in H_2 fumes exhibit greater total weight losses, primarily due to the shot blasting contribution. At the highest maximum temperature, the weight losses associated with shot blasting are comparable for both atmospheres, while pickling weight losses are higher for methane fumes. Overall, the pickling test on hot-rolled samples suggests

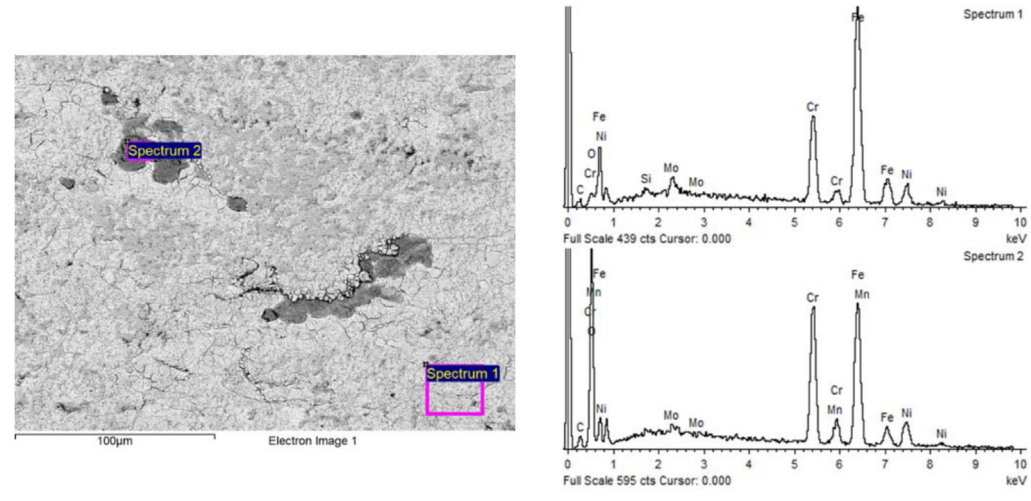

(a)

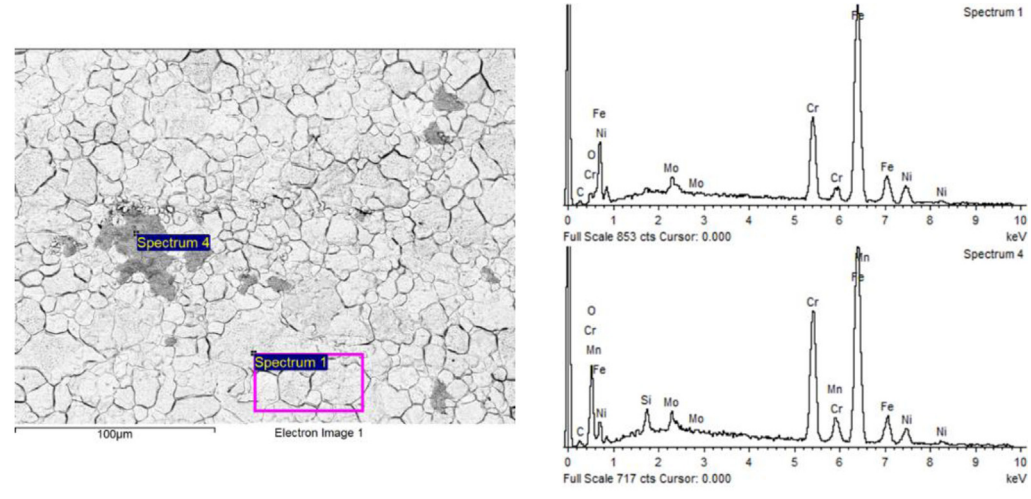

(b)

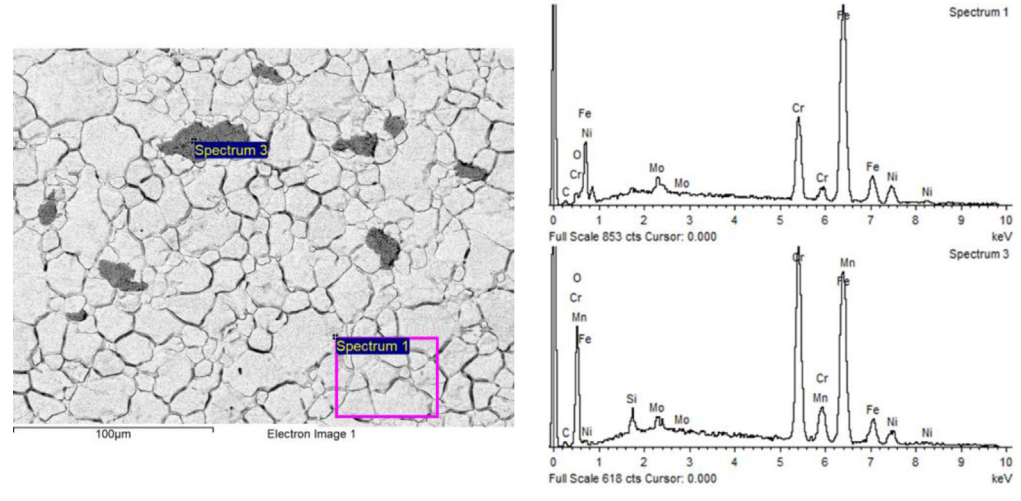

(c)

Fig. 13. EDX analysis after pickling treatment at minimum time of cold-rolled 316L samples annealed in atmosphere of CH_4 combustion fumes at maximum temperature of (a) 1080°C, (b) 1140°C, and (c) 1180°C and in atmosphere of H_2 combustion fumes at maximum temperature of (d) 1080°C, (e) 1140°C, and (f) 1180°C.

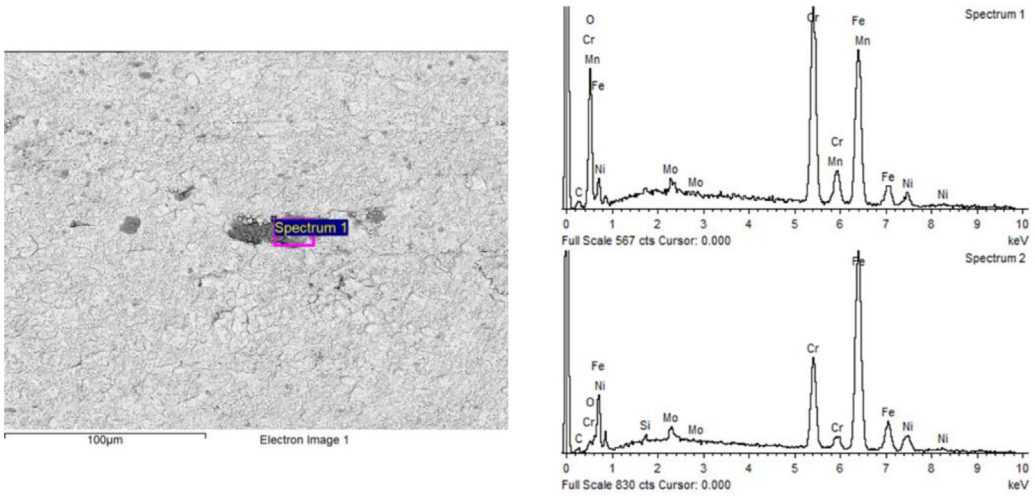

(d)

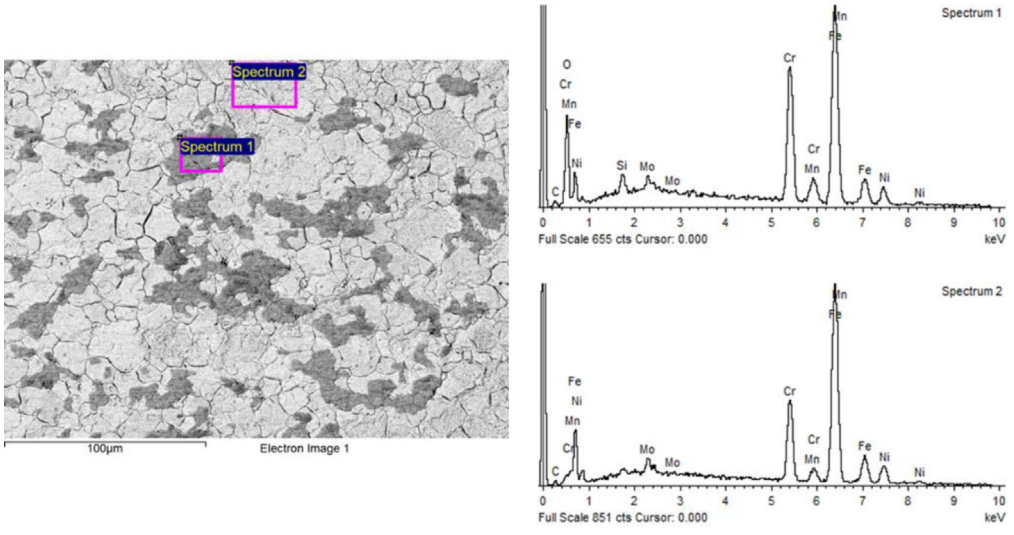

(e)

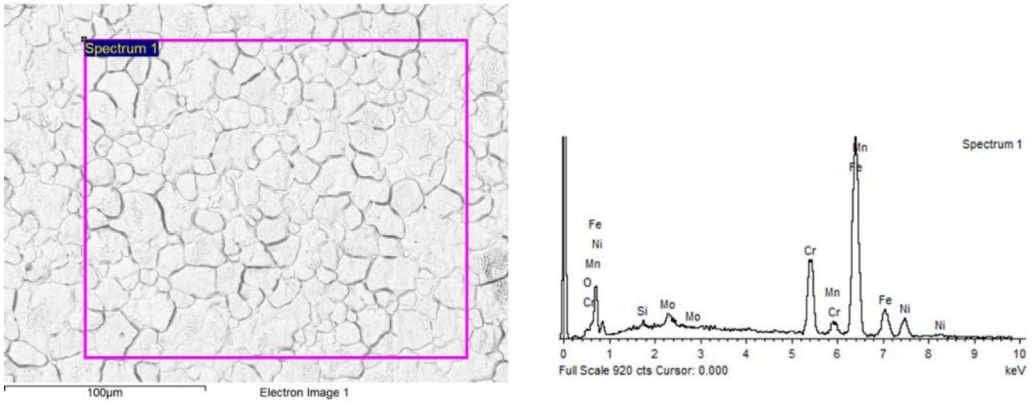

(f)

Fig. 13. (Continued)

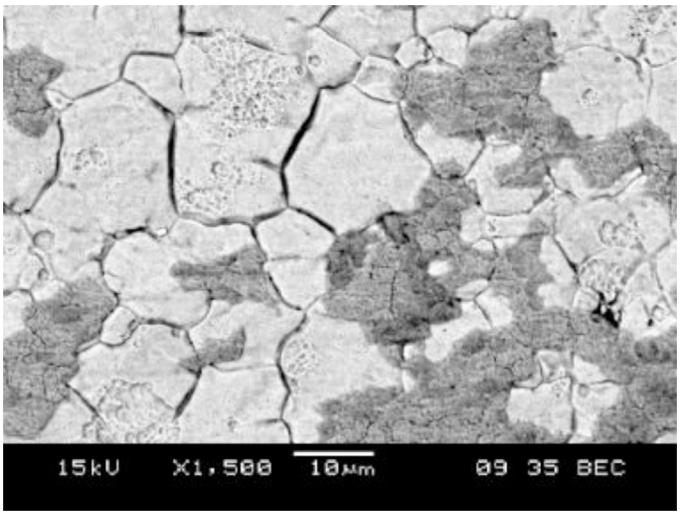

Fig. 14. SEM analysis at 1500× magnification of CR AISI 316L annealed in H_2 combustion fumes at 1140°C and subsequently pickled at the minimum pickling time.

that the use of hydrogen as a combustion fuel during the annealing process has a limited impact on the scale removal process.

4.2 Cold-rolled samples

Examining the cold-rolled and annealed sample with SEM, the surface appears completely oxidized. The oxide layers reflect the structure of the underlying base metal, preserving the grain boundaries that are visible as either thin lines or wider smudges. This effect might be correlated with a faster diffusion of chemical species through the grain boundaries, as noted by [13]. As the temperature increases, a notable phenomenon, scale detachment, becomes evident in both atmospheres. This leads to patches where the protective oxide layer peels away, exposing the metallic substrate beneath. EDX analysis of these exposed zones consistently shows a depletion of chromium, highlighting that chromium was depleted below the scale-metal interface.

Analysis of the GDOES experimental results demonstrates two trends: both oxide scale thickness and chromium depletion intensity increase with temperature, while hydrogen combustion atmospheres consistently produce more severe chromium depletion compared to methane atmospheres, though with only slightly thicker oxide scales. This is correlated with the accentuated volatile Cr hydroxide evaporation phenomenon. At the intermediate and high temperatures, the samples annealed in H_2 fumes show the formation of iron-rich oxide clusters. This phenomenon, which might be initiated by Cr evaporation, could be the onset of breakaway oxidation due to the less protective nature of iron oxides. Breakaway oxidation was, however, not observed due to the very short exposure time at high temperature. Although some authors found that Mo has a protective behavior [16] (enriching at the scale-metal interface), no such effect was visible.

The use of hydrogen as a combustion fuel reduces the minimum pickling time at both the lower and intermediate maximum annealing temperatures. At the highest maximum temperature no significant difference was observed between the two atmospheres. The weight losses show similar value in both annealing atmospheres. Overall, these findings indicate that the use of hydrogen as a combustion fuel does not substantially affect scale thickness or morphology and therefore has only a limited influence on the scale removal process. However, a comparison of SEM and EDX images for samples annealed in the two atmospheres shows that, at 1140°C, the specimen treated in hydrogen combustion fumes exhibits residual oxide and over-pickled areas, suggesting the formation of a locally more resistant oxide layer composed of Si and Mn, whose formation could be favored in H_2 combustion fumes.

5 Conclusion

For what concerns the oxidation process of hot-rolled and cold-rolled AISI 316L during annealing in methane and hydrogen combustion fumes, the following conclusions can be drawn from the results:

- Annealing in methane or hydrogen fumes has the effect of modifying the scale of hot-rolled materials. In both cases oxidation of the base metal and scale spallation take place. Hydrogen fumes, due to the higher water content, are more oxidizing and lead to higher oxide scale amounts. However, when annealing in hydrogen fumes, due to the chromium volatilization phenomena, which are enhanced by water vapor, the spallation is more effective compared to methane annealing. The spalled scale is found to consist mainly of Fe_3O_4 and Fe_2O_3. Atmosphere composition seems to have no effect on the chromium depletion phenomenon.
- The annealing in hydrogen fumes reduces or does not influence the pickling time of hot-rolled material. Moreover, it increases or does not influence the shot blasting contribution.
- Cold-rolled 316L is readily oxidized by both methane and hydrogen fumes. Oxide scale thickness increases with increasing temperature and is higher when annealing in

hydrogen fumes compared to methane fumes. Chromium depletion reaches a lower minimum Cr concentration when annealing in hydrogen fumes due to the chromium evaporation in a water vapor atmosphere. Iron oxide clusters appear on the surface of samples annealed at high temperature in H_2 fumes; this could be initiated by Cr evaporation and could be the onset of breakaway oxidation; however, breakaway oxidation did not occur due to the very short annealing time.
– The annealing in hydrogen fumes reduces or does not influence the pickling time of cold-rolled material. Moreover, it does not influence the overall weight losses.

Acknowledgments

The HR and CR stainless steels used in this work were provided by Marcegaglia S.p.A.

Funding

This research is part of the HYDRA project, which was funded by the Italian Ministry of Enterprises and Made in Italy (MIMIT) as part of the NextGenerationEU initiative.

Conflicts of interest

The authors have nothing to disclose.

Data availability statement

Only part of the data associated with this article can be disclosed due to legal and confidentiality reasons of Marcegaglia.

Author contribution statement

Conceptualization, E.S., L.C., N.M., and B.G.; Methodology, E. S., L.C., N.M., and B.G.; Formal Analysis, E.S., L.C., N.M.; Investigation, E.S., L.C., N.M.; Data Curation, E.S., L.C., N.M.; Writing–Original Draft Preparation, E.S., L.C., N.M.; Writing–Review & Editing, B.G.; Visualization, E.S., L.C., N.M.; Supervision, N.M. B.G.; Project Administration, B.G.

References

1. W. Nicodemi, Introduzione agli acciai inossidabili, AIM, 1995.
2. J. Callister, Materials Science and Engineering: An Introduction, Wiley, 2013.
3. K. Lo, C. Shek, J. Lai, Recent developments in stainless steels, Mater. Sci. Eng. **65**, 39–104 (2009).
4. WorldStainless, Stainless steel melt shop production increases by 7% in 2024, 14 April 2025. [Online]. Available: https://worldstainless.org/media/press-releases/stainless-steel-melt-shop-production-increases-by-7-in-2024/. [Accessed 17 Nov 2025]
5. B. Ozturk, R. Matway, Oxidation of type 304 stainless steels under simulated annealing conditions, ISIJ Int. **37**(2), 169–175 (1997).
6. S. Saunders, M. Monteiro, F. Rizzo, The oxidation behaviour of metals and alloys at high temperatures in atmospheres containing water vapour: a review, Prog. Mater. Sci. **53**, 775–837 (2008).
7. S. Gonzales, L. Combarmond, M. Thi Tran, et al., Short term oxidation of stainless steels during final annealing, Mater. Sci. Forum, **2595–2598**, 601–610 (2008).
8. R. Jargelius-Petterson, P. Szakalos, Oxidation of type 304 stainless steel during annealing, Swedish Inst. Metals Res., 347–348.
9. C. Wagner, Theoretical analysis of the diffusion processes determining the oxidation rate of alloys, J Electrochem. Soc. **99**, 369–380 (1952).
10. L. Fernando, D. Zaremski, Some fundamental aspects of snnealing and pickling stainless steels, Metall. Transac. A **19A**, 1083–1100 (1988).
11. C. Gindorf, L. Singheiser, K. Hilpert, Vaporization of chromia in humid air, J Phys. Chem. Solids **66**, 384–387 (2005).
12. K. Segerdhal, J. Svensson, M. Halvarsson, et al., Breakdown of the protective oxide on 11% Cr steel at high temperature in the presence of water vapor and oxygen, the influence of chromium vaporization, Mater. High Temp. **22**, 69–78 (2005).
13. H. Asteman, K. Segerdahl, J. Svensson, et al., Oxidation of stainless steel in H2O/O2 environments—role of chromium evaporation, Mater. Sci. Forum **461-494**, 775–782 (2004).
14. S. Airaksinen, A. Laukka, E.-P. Heikkinen, et al., From fossil-fueled to hydrogen-fueled annealing furnaces: effects of the oxidation of stainless steels, Steel Res. Int., **94** (2023).
15. V. Badin, E. Diamanti, P. Foret, et al., Water vapor oxidation of ferritic 441 and austenitic 316L stainless steels at 1100°C for short duration, Procedia Mater. Sci. **9**, 48–53 (2015).
16. H. Buscail, S. El Messki, F. Riffard, et al., Role of molybdenum on the AISI 316L oxidation at 900°C, J. Mater. Sci. **43**, 6960–6966 (2008).
17. R. Bartlett, Molybdenum oxidation kinetics at high temperatures, J. Electrochem. Soc. **112-7**, 744–746 (1965).
18. A. Nelson, E. Sooby, Y. Kim, et al., High temperature oxidation of molybdenum in water vapor environments, J. Nucl. Mater. **448**, 441–447 (2014).
19. D. Henriet, Surface treatments for stainless steel state of the art—developments and trends, European Commission, Brussels, 1995.
20. S. Chandra-ambhorn, P. Wongpromrat, T. Thublaor, et al., Effect of water vapor on the high temperature oxidation of stainless steel, Solid State Phenom. **300**, 107–134 (2020).

Cite this article as: Eugenia Sainsus, Lorenza Catini, Niccolò Massarelli, Baldo Gurreri, Effect of Hydrogen as fuel for continuous annealing of AISI 316L stainless steel—annealing and pickling tests, Matériaux & Techniques **114**, 308 (2026), https://doi.org/10.1051/mattech/2026017